



Hydrogeochemistry and evaluation of groundwater suitability for irrigation purpose in the Mornag region, northeastern Tunisia

Amor Ben Moussa^{1,2,3} · Sawsan Chandoul² · Houcem Mzali⁴ · Sarra Bel Haj Salem¹ · Hatem Elmejri¹ · Kamel Zouari⁵ · Amor Hafiane² · Habib Mrabet⁶

Received: 17 July 2019 / Accepted: 17 March 2020 / Published online: 20 March 2020
© Springer Nature B.V. 2020

Abstract

In semiarid regions, salinization and anthropogenic contaminants are considered as the principal threat to groundwater resource availability. Consequently, the origin and processes of salinization should be identified, to take a sustainable measurement to mitigate these problems. In the present study, groundwater samples from 18 dug wells were collected during the sampling campaign carried out in May 2016 in order to identify the main natural and anthropogenic processes that control the quality of groundwater in the Mornag shallow aquifer (northeastern Tunisia) and to evaluate its suitability for agricultural irrigation purpose. This may create a clear database for decision maker to take suitable actions to sustainably manage the groundwater resources. The hydrogeochemical parameters (major ions concentration, pH, TDS, EC) were examined to assess the quality of groundwater and to identify the main mineralization processes. Permeability index (PI), percentage of sodium (%Na) and the ratio of sodium adsorption (SAR) were investigated to evaluate the groundwater suitability for irrigation. It has been demonstrated that the major ions abundance follows the order of sodium > calcium > magnesium > potassium and chloride > sulfate > bicarbonate > nitrate. Dissolution of evaporite minerals, such as halite, gypsum and anhydrite, and reverse ion exchange are the predominant processes of groundwater mineralization, generating the Cl–SO₄–Ca and Na–Cl major water types. The calculated irrigation water quality index displayed that 55% of the Mornag groundwater samples are distinguished by elevated SAR and PI, suggesting their unsuitability for irrigation. So, the present study has provided a precious insight into the major geochemical processes occurring in the Mornag shallow groundwater and their suitability for irrigation which will support future management of these resources.

Keywords Mornag region · Quaternary aquifer · Mineralization processes · Dissolution of evaporate · Water quality · Unsuitable for irrigation

✉ Amor Ben Moussa
amor_geologic@yahoo.fr

Extended author information available on the last page of the article

1 Introduction

Groundwater is the main source of public water supplies not only in housing but also in industrial and agriculture activities (Kalaivanan et al. 2018; Amin et al. 2018). The quantity and quality of groundwater have become a major challenge faced by many regions today. Indeed, the fast population growth as well as the socioeconomic development has resulted in increasing demands for water resources. It is reported that these activities have resulted in several long-term effects on groundwater resources such as a general decline in water levels, an increase in the risk of saltwater intrusion and water quality degradation. In arid and semiarid regions, groundwater pollution can lead to a vast array of environmental, social and economic consequences added to the impacts on health and livestock (Toumi et al. 2015). In Mornag region, for instance, located to the northeast of Tunisia, the shallow groundwater aquifer showed significant qualitative and quantitative changes (Lassoued et al. 1995). These changes are manifested through a general decline in the level of water table and the degradation of water quality (Chandoul 2017). Moreover, the deterioration of groundwater quality, which is considered as an expected side effect of the aquifer over-exploitation, represents another major problem for decision makers and managers (Farhat 2011). Indeed, groundwater quality, which is influenced by both natural and anthropogenic mineralization processes, needs to be considered as a fundamental element for a sustainable management. Understanding the hydrodynamic functioning and the evolution of groundwater geochemical composition is what guarantees the effectiveness and sustainability of decisions that should be taken for the management of water resources.

Therefore, it is essential to understand groundwater hydrodynamic functioning and to identify the mineralization processes of Mornag coastal aquifer when assessing the possible risks that may result from the quantitative and qualitative degradation of shallow groundwater. The present investigation aims at providing the appropriate information about the hydrodynamic behavior of the studied aquifer, the dominant geochemical processes that control groundwater quality and how useful and suitable it is for irrigation purposes.

2 Study area

The Mornag region with a land area of about 370 km² is located on the northeastern part of Tunisia within latitudes 36° 34' to 36° 46' N and longitudes 10° 6' to 10° 24' E (Fig. 1). It is bounded by the Gulf of Tunis in the north, Jebel Boukornine in the northeast, Jebel Ressaas and Jebel Hmadet el Khafi in the south and the hills of Rades, Megrine and BirKassâa in the west. Land-surface altitude of the highest mountain is 795 m a.s.l on the Ressaas Mountain. The major economic activity in the Mornag plain, which has the most fertile land in Tunisia, is agriculture with principal crops being citrus and vine. Moreover, the study region is known by its industrial activity with companies that operate mainly in the mechanical, electrical, and textile, leather and clothing industries.

The climatic study, which was carried out based on the data recorded at the Mornag CTV weather station during the last 15 years, shows that the climate of the study district is classified as Mediterranean. It is characterized by relatively hot, dry summer and mild winter (Chandoul 2017). The study area is dominated by winds from the east, in summer, northeast, in the spring and west and northwest in winter (Bargaoui 1983). December is the wettest month with a maximum rainfall of 80 mm, and the driest month is July with a

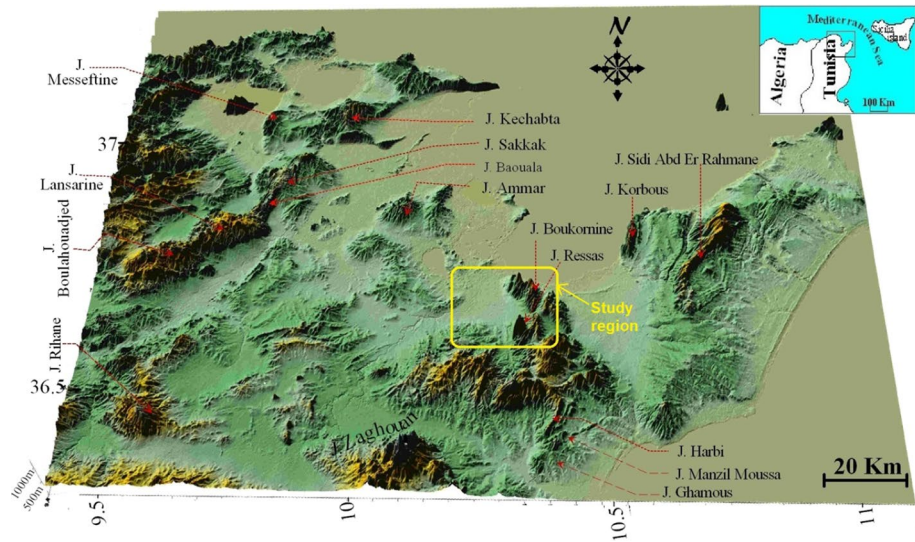


Fig. 1 Digital elevation model of the northeastern Tunisia, showing the location of the study region

mean rainfall of about 5 mm. The annual precipitation averages at 550 mm. The maximum temperatures usually exceed 31 °C during the summer, precisely in August, and the lowest mean minimum occurs in January with 10 °C. The mean annual potential evapotranspiration exceeds 1700 mm/year.

The hydrographic network in the Mornag plain is represented by wadi Meliane which drains a catchment covering an area of about 1996 km². Wadi Meliane, which is the major wadi in the study area, is the second permanent wadi of Tunisia, after the Medjerda extending over a length of 100 km. It flows from the southwest to the northeast along the axis of the plain, collecting surface rainwater from the foot of Djebel Bargou toward the Gulf of Tunis. Moreover, the region is fed by canal derived from Medjerda wadi. This wadi is characterized by an irregular annual average rate varying largely between 5×10^6 and 200 m³/year (BRLI 2007).

3 Geologic and hydrogeologic setting

The Mornag plain consists mainly of Quaternary sediments which are of great hydrologic importance. These deposits are bounded by the Late Miocene deposits to the northwest, by the Paleogene deposits to the southeast and by sediments of age spread from Triassic to Late Eocene to the East (Bujalka et al. 1971; Vacek et al. 1971) (Fig. 2). The most important outcrops of Sediments belonging to Triassic—Late Cretaceous interval appear in the east of the study region. Paleocene sediments crop out in the south and the southeast. Eocene deposits crop out in the south, in the east of Jebel Ressay and in the west of Jebel Boukornine. Oligocene sediments appear in the south and in the central west and Miocene sediments crop out in the northwest (Fig. 2). In the northeast of Tunisia, sedimentation from Triassic to Quaternary is characterized generally by gypsum, clays, limestone, marls and sandstone (Fig. 3) (Burolet 1956; Florida and Massin 1969; Rakus and Biely 1971;

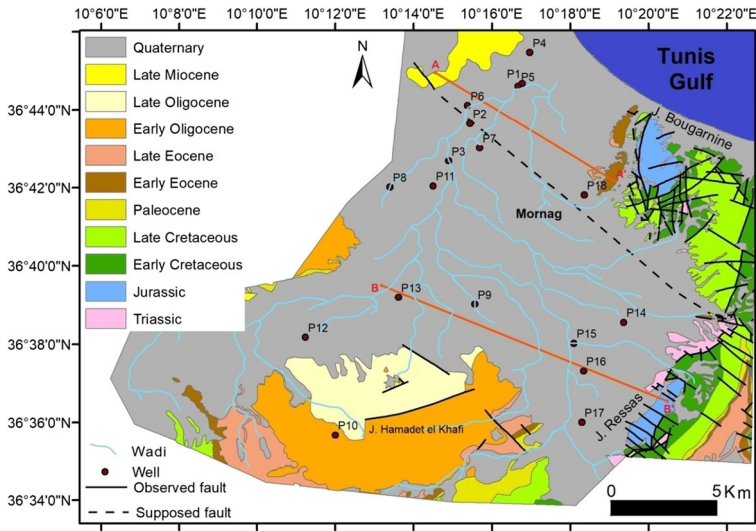


Fig. 2 Geological map of the study region (Bujalka et al. 1971; Vacek et al. 1971)

Bujalka et al. 1971; Biely et al. 1972; Bonnefous 1972; Bouhlel 1982; Turki 1985; Bismuth and Hooyberghs 1994; Soussi et al. 2000; Mzali and Zouari 2012; Amri et al. 2018).

Triassic series consist of gypsum, clay, sandstone and dolomite. Jurassic deposits are represented by limestone and marls. Early Cretaceous sediments consist of consolidate sandstone with marls at the base which are situated beneath marly limestone, limestone and marls. Late Cretaceous sediments are characterized by limestone at the base which are overlain by clays and alternation of clays and marly limestone banks and by limestone bar and marls at the top. Paleogene deposits are characterized by marls of Paleocene, limestone of Early Eocene, clays intercalated by a limestone bar of Late Eocene, alternations of clays and sandstone of Early Oligocene and sandstone of Late Oligocene. Late Miocene sediments consist of clays and sandstone alternations overlain by sands at the top. In the north-east of Tunisia, Quaternary deposits are generally continental. Indeed, Marine sediments appear in the Cap Bon peninsula (Moussa et al. 2014). In the study region, Quaternary sediments are represented by sands, red clays, sandy clays, consolidates dunes, soils, scree, gravel, clay and conglomerate (Bujalka et al. 1971).

The Mornag plain is situated in the Tunisian Atlas which is characterized by compound deformations that are represented by faults of different directions, NW–SE-oriented collapse structures and NE–SW-oriented folds (Ben Haj Ali et al. 1985). This plain is limited to the east by the Zaghouan fault where its play as a thrust fault resulted in the building of the Tunisian dorsal (Turki 1985).

Quaternary sediments of the Mornag plain cover two different compartments which are separated by a NW–SE-oriented fault. The northern compartment is characterized by a sedimentary gap between Oligocene and Early Miocene deposits and is part of a syncline structure where the dip layers are 60° toward the northwest in the southeast flank and 25° toward the southeast in the northwest flank (Fig. 2). Quaternary sediments of this compartment lie with angular unconformity on the Late Eocene and Middle to Late Miocene deposits. The southern compartment is characterized by a complete stratigraphic series, and it forms a syncline structure with a relatively symmetric flank. Quaternary sediments

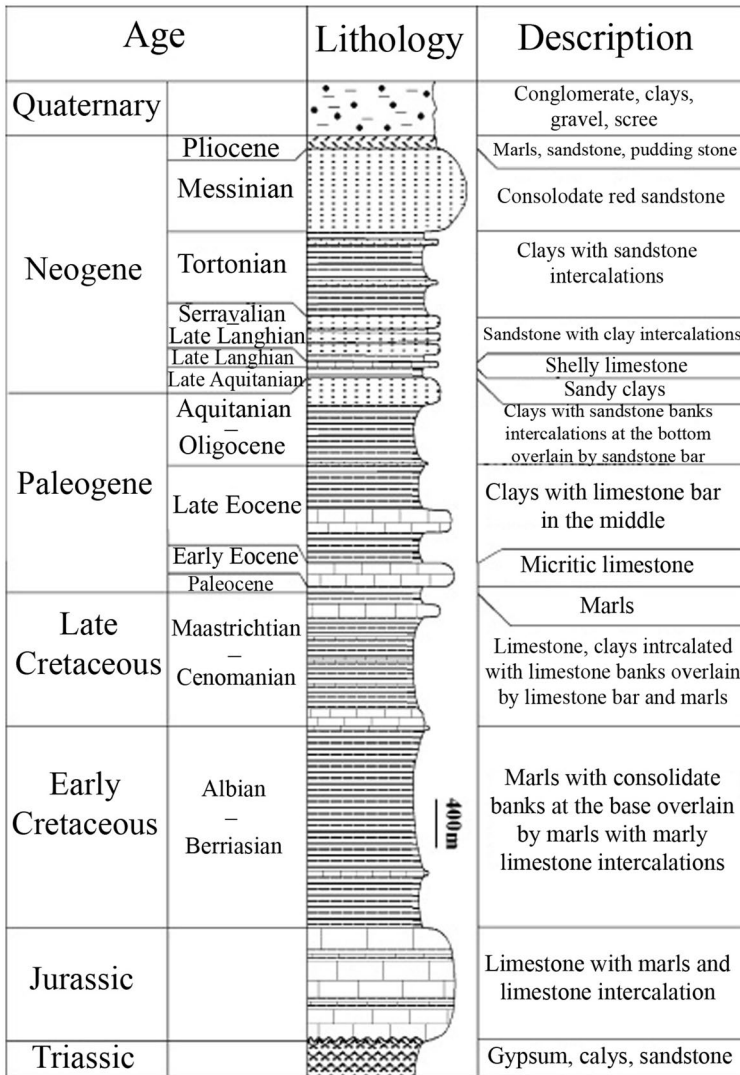


Fig. 3 Synthetic stratigraphic column of the study region (Mzali and Zouari 2012)

of this compartment lie with angular unconformity on the Triassic, Late Cretaceous, Paleocene, Eocene, Oligocene and Miocene deposits (Fig. 3). The difference in the two compartments is the result of the activity of the NW–SE fault, which separates them, during the extensive and compressive tectonic phases.

Quaternary deposit thickness varies along the Mornag plain. Indeed, water wells drilled in this plain show thicknesses varying from 13 m to almost 250 m (Farhat 2011). The maximum thickness of the Quaternary sediments is shown in the syncline core (Fig. 4).

Previous regional hydrogeologic investigations indicate that the Mornag plain contains a complex multi-level aquifer system (Lajmi 1968; Ennabli 1980; Hechemi 1989; Farhat

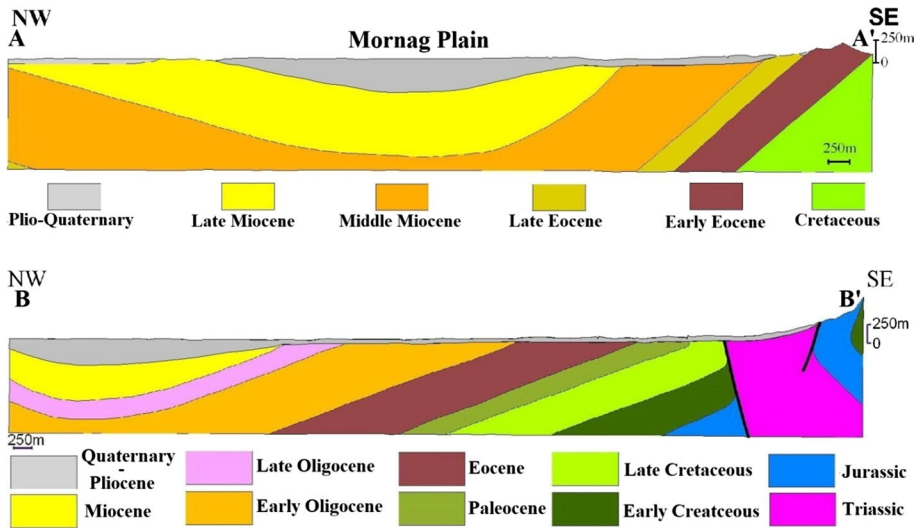


Fig. 4 Geological cross section (A–A' and B–B') showing deformations geometry in the northern and southern compartments of Mornag plain

2011; Mezrioui 2015). The shallow aquifer, which is the uppermost hydrogeologic unit, includes sediments of Quaternary age (Fig. 4). It consists mostly of alluvial deposits with variable amounts of sandstone, sand, sandy clay and clay. This aquifer, which is unconfined in the entire study area, has a synclinal structure and lies in angular discordance on the underlying sedimentary series. Recharge to the Quaternary shallow aquifer is mainly from the precipitation that infiltrates at the foot of the bordering hills, in the Khlédia, Ettella and Rorouf regions. Thickness of the Mornag shallow aquifer ranges from a 10 m to greater than 30 m in the central part of the plain. Hydraulic conductivity for the shallow unconfined aquifer is estimated to range from 0.5×10^{-5} to 2×10^{-3} m/s, and the transmissivity values range from less than 10^{-4} m²/s to greater than 80×10^{-4} m²/s (Farhat 2011; Chandoul 2017).

A piezometric map of the Mornag shallow aquifer was prepared from water-level measurements made during May 2016 (Fig. 5). This map shows that measured water levels were about 70 m, in the southern part of the basin, to about 10 m, the northern part, and closer to the Gulf of Tunis. Groundwater generally follows topography, showing a general flow pattern from mountainous areas, in the south, toward the Mediterranean Sea, in the north. The hydraulic gradient typically follows topography. Regions with high hydraulic gradients, indicated by higher density of potentiometric contours, may reflect either reduction in the hydraulic conductivity or reduction in the more permeable zones within the aquifer.

4 Materials and methods

The present investigation, which reveals the hydrochemical criteria in the Mornag plain, is conducted to characterize, understand and interpret groundwater mineralization in the regional context. As shown in Fig. 2, a total of 18 samples of shallow groundwater were collected from shallow wells. All samples were stored in washed polypropylene bottles

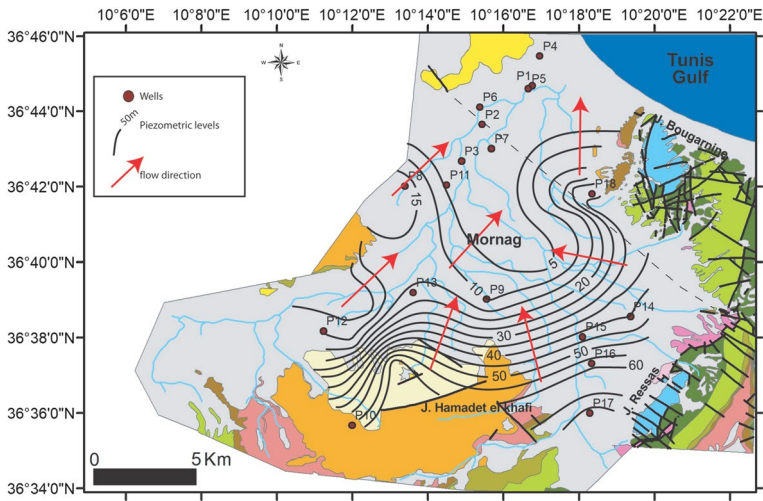


Fig. 5 Piezometric map of the Mornag shallow aquifer

to avoid unpredictable changes in characteristic. Physicochemical parameters, such as electrical conductivity (EC), pH and temperature (T °C), were measured in the field, directly after sample collection using a portable multi-parameter. Major cations (Ca^{2+} , Mg^{2+} , Na^+ , K^+) and anions (Cl^- , SO_4^{2-} , HCO_3^- , NO_3^-) concentrations were measured in the “Laboratoire de Radio-Analyses et Environnement” of the Engineers School of Sfax, Tunisia. These measurements were taken on a water ion chromatograph using IC-PakTMCM/D columns, for cation, and a water ion chromatograph (Metrohm) using CI-SUPER-SEP columns, for anion. Concentrations of major ions were converted to milliequivalents per liter, and the analytical precision to the measurement is about $\pm 5\%$. The ionic charge balance error was below 5%, which is within the acceptable limit (Domenico and Schwartz 1990; Freeze and Cherry 1979). Groundwater quality indexes such as percentage sodium (%Na), permeability index (PI) and sodium absorption ratio (SAR) were used to evaluate irrigation water quality (Table 1). Surfer 9 software has been used to establish different spatial distribution maps of various chemical ions and indexes in the Mornag shallow groundwater.

Table 1 Equations used for calculation of water quality indices in Mornag groundwater samples

Water quality indices	Equations	Unit	References
Sodium absorption ratio (SAR)	$\text{SAR} = \frac{\text{Na}}{\sqrt{\frac{\text{Ca} + \text{Mg}}{2}}}$	meq/L	Richards (1954)
Percent sodium (%Na)	$\% \text{Na} = \frac{\text{Na} + \text{K}^+}{(\text{Ca}^{2+} + \text{Mg}^{2+} + \text{Na}^+ + \text{K}^+)} \times 100$	%	Wilcox (1955)
Permeability index (PI)	$\text{PI} = \frac{\text{Na} + \sqrt{\text{HCO}_3^-}}{(\text{Ca}^{2+} + \text{Mg}^{2+} + \text{Na}^+)} \times 100$	meq/L	Doneen (1964)

5 Results and discussion

5.1 Aquifer geochemistry

5.1.1 Ions concentration

Understanding the aquifer hydrochemistry is essential to recognize origins of groundwater and the mineralization processes which occur in the Mornag aquifer. The groundwater hydrochemical data of Mornag shallow unconfined aquifer are shown in Table 2. Total dissolved solid (TDS) concentrations in the Mornag unconfined groundwater displays a wide range of variation from 0.8 to 11.6 g/L. The electrical conductivity (EC) values, which vary from 1154 to 11000 $\mu\text{S}/\text{cm}$, are function of the total dissolved solids (TDS). In fact, the spatial distribution of the TDS and EC shows that low values have been recorded in the foot of the surrounding hills, suggesting the effect of recharge by rainfall fresh water (Fig. 6a, b). The central and northern parts of the basin are distinguished by moderate to high values of TDS and EC, highlighting the impact of the water–rock interaction enhanced by the residence time and the anthropogenic activities (agriculture and industry). However, the maximum value of TDS (11.6 g/L) has been reported in the southeastern part of the study area, lending support to the groundwater interaction with salt Triassic sediments which outcrops in the foot of Jebel Ressas. The Mornag unconfined groundwater displays pH values that vary from 6.8 to 8.25, indicating that groundwater is generally alkaline, highlighting the combined effect of numerous geochemical and biological processes. Indeed, biological activities can generally accelerate geochemical processes.

The major ions mean abundance in the Mornag unconfined groundwater follows the order of $\text{Na}^+ > \text{Ca}^{2+} > \text{Mg}^{2+} > \text{K}^+$, for the cations, and the order of $\text{Cl}^- > \text{SO}_4^{2-} > \text{HCO}_3^- > \text{NO}_3^-$, for the anions. This is confirmed by the position of groundwater samples in the Piper plot, suggesting that the majority of the groundwater chemistry consists of Na^+ , Ca^{2+} , Cl^- and SO_4^{2-} (Piper 1944). Indeed, sodium is the dominant cation with about 57% of all the cations, while calcium and magnesium are of 28.7 and 11.5%, respectively. Chloride is dominant anion representing 50% of all the anions, whereas sulfate and bicarbonate are of 20 and 28%, respectively. Consequently, based on Piper diagram, Mornag groundwater samples can be classified into two major water types such as $\text{Cl}-\text{SO}_4-\text{Ca}$ and $\text{Na}-\text{Cl}$ facieses (Fig. 7). Correlations between the sum of cations, the sum of anions and majors ions are helpful in determining the principal chemical elements that contribute to the groundwater mineralization and identifying geochemical processes that occur in the aquifer. The present investigation shows that there are positive correlations in the plots of Na^+ , Ca^{2+} and Mg^{2+} versus the sum of cations and in the plots of Cl^- and SO_4^{2-} versus the sum of anions, indicating their considerable contribution to the groundwater mineralization processes (Fig. 8). Furthermore, qualitative and quantitative insights about mineralization processes controlling Mornag groundwater can be obtained using Gibbs diagrams (Gibbs 1970). Indeed, Gibbs diagrams can bring reliable information about precipitation, rock interaction and evaporation processes that control groundwater composition. Gibbs plots highlight that water–rock interaction is the principal processes influencing the Mornag groundwater composition, especially in the southeastern part of the study area (Fig. 9). However, some groundwater samples deviate from the domain of rock dissolution and lending support to the effect of the evaporation process on groundwater quality.

Table 2 In situ measurements and geochemical data of Mornag shallow groundwaters

Well number	pH	CE ($\mu\text{s}/\text{cm}$)	Na^+	K^+	Ca^{2+}	Mg^{2+}	HCO_3^-	Cl^-	NO_3^-	SO_4^{2-}	TDS	Chloro-alkaline index				
												CA11	CA12	Saturation indexes		
													Gypsum	Anhydrite	Halite	
P1	8.24	4270	565.05	25.6	177.35	76.85	439.2	894	<0.01	529.85	2707.9	0.36	0.24	-0.91	-1.13	-4.96
P2	8	4480	583.7	20.4	195.9	90.35	359.9	969.5	<0.01	578.5	2798.25	-0.50	-0.25	-0.85	-1.07	-4.92
P3	7.89	4800	778.8	31.2	250.7	125.95	414.8	1358.75	<0.01	807.8	3768	0.19	0.77	-0.69	-0.91	-4.66
P4	8.2	2980	412.8	23.6	146.8	72.43	390.4	542.53	<0.01	476.25	2064.8	0.48	1.32	-0.96	-1.2	-5.29
P5	6.82	6770	872.6	8.15	348.95	179.4	475.8	1652.75	18.35	953.9	4509.9	0.10	0.15	-0.53	-0.77	-4.53
P6	7.01	6560	811.3	3.3	446	206.65	518.5	1433.05	0	1413.05	4831.85	-0.21	-0.20	-0.31	-0.55	-4.64
P7	7.28	3330	368.78	2	224.05	98.2	524.6	493.65	14.4	678.9	2404.58	0.51	0.80	-0.7	-0.93	-5.39
P8	7.05	1890	217.99	18.69	97.13	44.82	488	235.4	28.29	242.65	1372.97	-0.16	-0.09	-1.3	-1.53	-5.9
P9	8	2210	217.44	3.32	172.88	58.6	427	365.22	46.24	248.62	1539.32	0.10	0.11	-1.1	-1.34	-5.72
P10	8.15	5520	476.55	30.8	481.7	195.85	616.1	1467.5	<0.01	239.15	3507.65	0.23	0.24	-0.96	-1.2	-4.83
P11	7.15	6410	794.15	5.85	360.2	235.05	451.4	1368.45	129.6	1190.1	4534.8	0.13	0.13	-0.46	-0.69	-4.66
P12	7.47	1767	151.75	4.26	113.25	62.69	347.7	321.54	51.25	120.12	1172.56	0.07	0.06	-1.52	-1.76	-5.92
P13	7.8	2870	187.4	17.93	272.63	73.4	311.1	625.03	164.95	171.88	1824.3	0.18	0.30	-1.13	-1.37	-5.57
P14	6.82	1154	65.42	3.89	125.93	32.21	244	161.99	88.06	61.94	783.44	0.05	0.08	-1.68	-1.92	-6.57
P15	6.82	11000	2838.3	124	869.7	254	317.2	5564.6	24.6	1621.7	11614.1	0.00	0.00	-0.14	-0.26	-7.57
P16	7.65	2080	291.13	3	268.6	59.6	359.9	583.43	55.45	427.55	2048.65	0.23	0.13	-0.8	-0.94	-5.46
P17	7.47	1767	150.88	3.04	256.1	67.08	347.7	307.4	<0.01	499.76	1631.96	0.26	0.26	-0.72	-0.91	-5.99
P18	7.7	1300	102.04	9.67	107.57	41.04	353.8	233.34	<0.01	83.95	931.41	0.29	0.25	-1.67	-1.84	-6.26

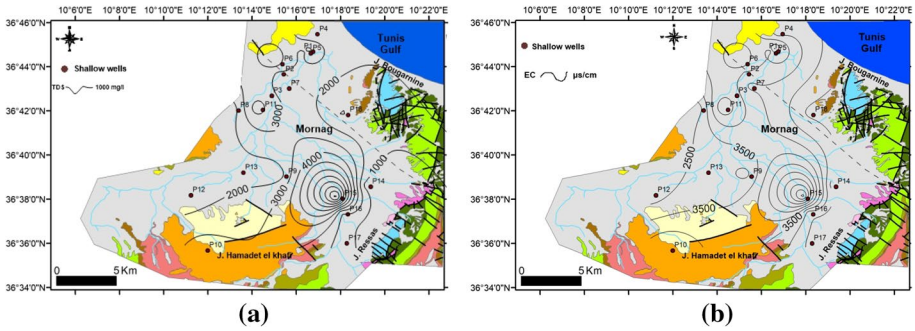
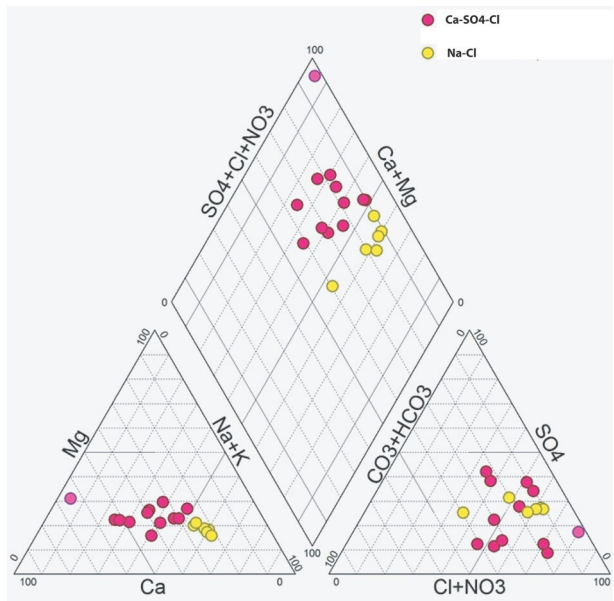


Fig. 6 Spatial distributions of TDS (a) and electrical conductivity (b)

Fig. 7 Piper diagram of the Mornag shallow groundwaters



In order to highlight more in detail these mineralization processes, various bivariate conventional diagrams between major ions have been examined in conjunction with saturation indexes versus some minerals. In the plot of Na versus Cl most groundwater samples from the Mornag shallow aquifer fall along the 1:1 line (Fig. 10a). Moreover, the spatial distribution maps of sodium and chloride show that the concentrations of these two ions increased in the same direction of groundwater flow (Fig. 11a, b). This may be related to the halite (NaCl) dissolution, which is highlighted by the negative values of saturation indexes (Table 2). These later suggest an under-saturation state with respect to NaCl mineral and consequently its likely dissolution (Moussa et al. 2017). The Ca versus SO₄ diagram displays well-defined relationship between calcium and sulfates, suggesting that these ions derive from the dissolution of gypsum and/or anhydrite minerals (Fig. 10b). The dissolution of sulfate minerals is in concordance with both the under-saturation state of the Mornag shallow groundwater with respect to the gypsum and anhydrite minerals and the

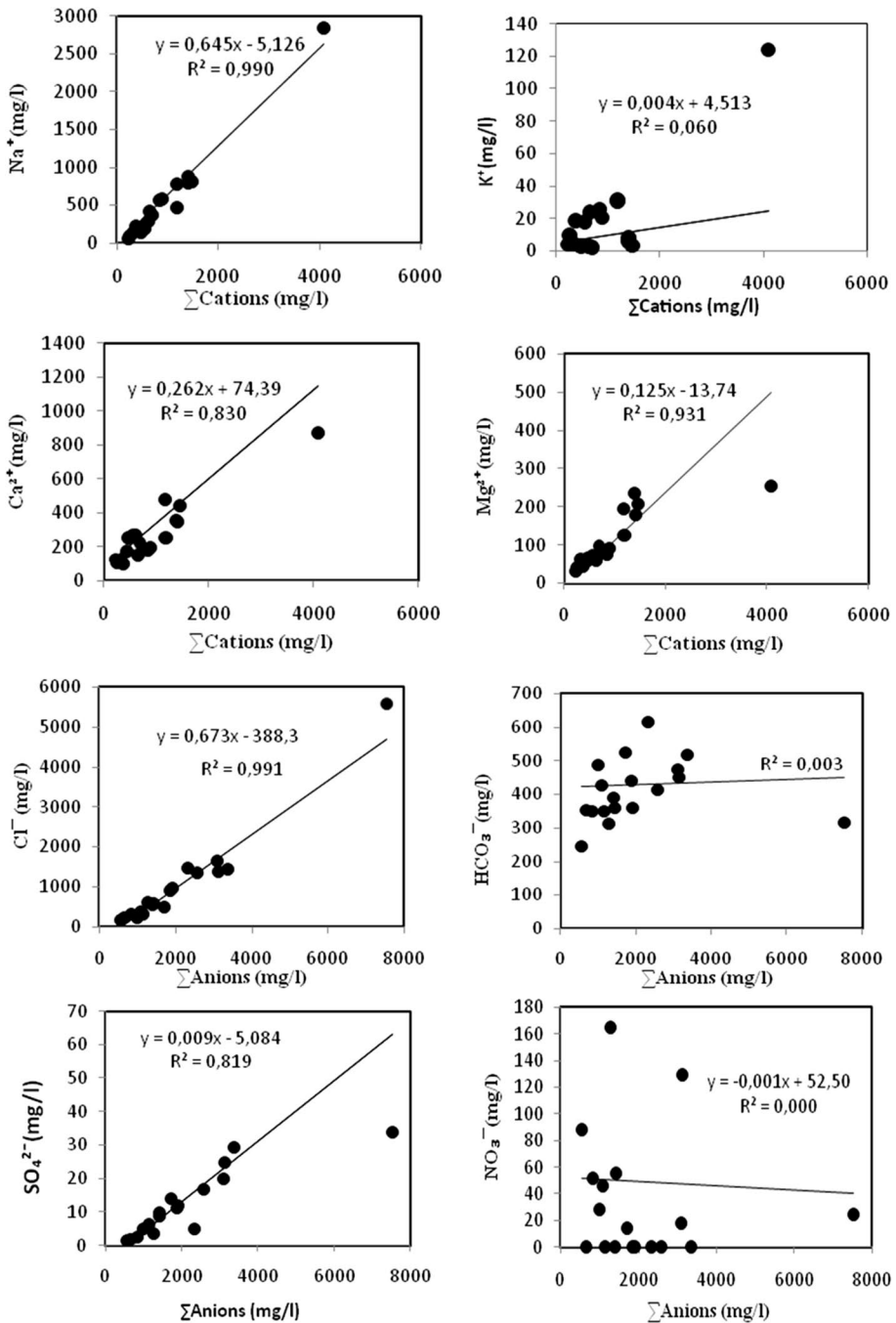


Fig. 8 Plots of Σ anions versus each anion and Σ cations versus each cation

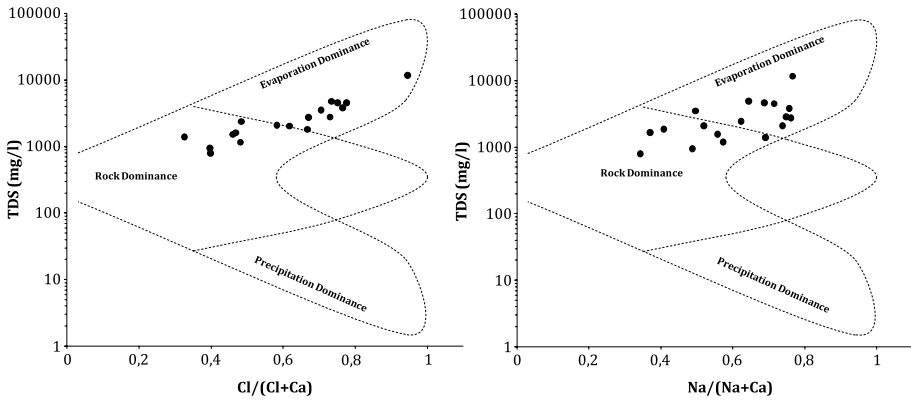


Fig. 9 Gibbs plots explain groundwater geochemical process in the Mornag region

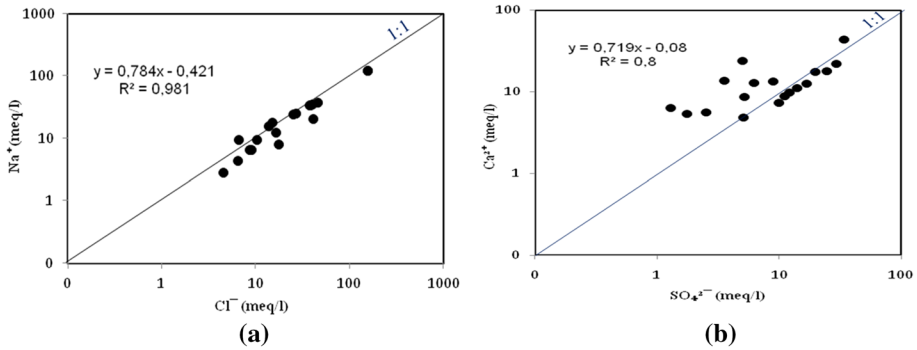


Fig. 10 Plots of Na versus Cl (a) and Ca versus SO₄ (b)

similar spatial evolution of calcium and sulfates concentrations, which increase conformably to the direction of groundwater flow (Fig. 11c, d). However, some groundwater samples are distinguished by a deficit of sodium which corresponds to an excess of calcium. This observation may be explained by the effect of ions exchange with clayey mineral relatively abundant in the Mornag unconfined aquifer. Additionally, the estimation of the ion exchange indexes displays positive values indicating reverse cation exchange, where Na⁺ and K⁺ from water are exchanged with Mg²⁺ and Ca²⁺ in clay minerals (Moussa and Zouari 2011) (Table 2). Figure 12 highlights the occurrence of cation exchange process in the Mornag shallow aquifer. This plot shows that groundwater samples fall along a line with a slope of -1, confirming that cation exchange is an important process, which plays a fundamental role in the modification of groundwater geochemical composition (Dassi et al. 2005; Kamel et al. 2006; Tarki et al. 2016; Moussa et al. 2017).

5.1.2 Nitrate concentrations

Groundwater samples display a broad range of nitrate contents, which vary from below the detection limit to 164.95 mg/L. Among 18 groundwater samples, six samples are

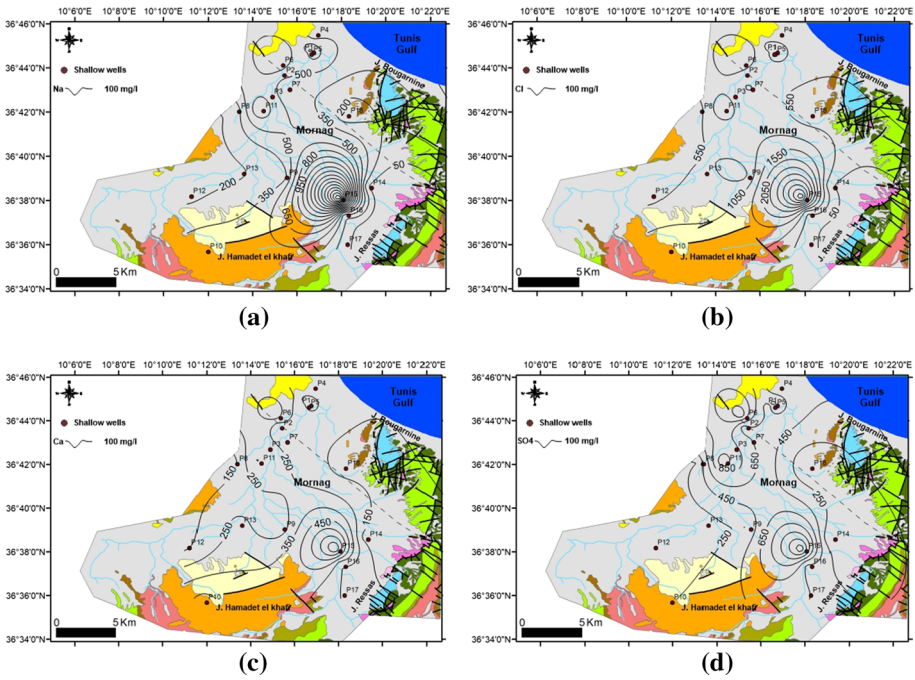


Fig. 11 Spatial distributions of Na (a), Cl (b), Ca (c) and SO₄ (d)

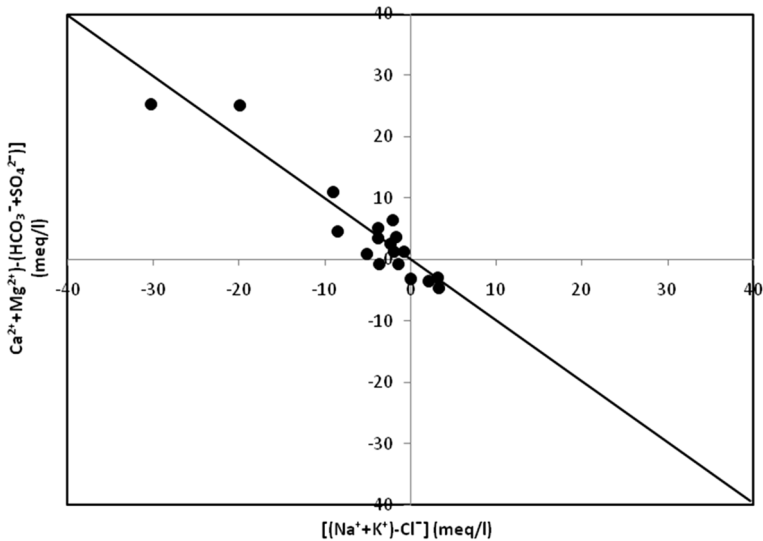


Fig. 12 Plot of $(Na^+ + K^+ - Cl^-)$ versus $[(SO_4^{2-} + HCO_3^-) - (Ca^{2+} + Mg^{2+})]$

distinguished by nitrates contents above the recommended World Health Organization limit for NO₃ in drinking water, estimated to 50 mg/L (WHO 2011). The examination of nitrate concentration variations with respect to well depth suggests that nitrate contents in

the Mornag shallow aquifer decrease likely with increasing well depth. The higher NO_3 concentration may reflect the effect of anthropogenic contamination related to agricultural and industrial activities (Moussa et al. 2008). The mapped spatial distribution displays that highest NO_3 contents (above 50 mg/L) were found in the central part of the Mornag plain which are distinguished by intensive farming production (Fig. 13). Indeed, the excessive use of chemical fertilizer represents a major factor contributing to the increase in N concentration in groundwater through return flow of irrigation water. Moreover, other source of nitrates originates from industrial waste water, especially in the eastern part of the study area. In this region, the infiltration of wastewater throughout the Meliane wadi plays a fundamental role in increasing the contamination of groundwater by nitrate.

5.2 Groundwater suitability for irrigation

The assessment groundwater suitability for irrigation purpose in the Mornag region was carried out basing on electrical conductivity, sodium adsorption ratio (SAR), % sodium and permeability index (PI). It is essential to evaluate the quality of water available for irrigation, depending on the aforementioned parameters for a successful application and beneficial uses. Indeed, inadequate evaluation of the irrigation water quality can result in soil structure degradation and plants production problems, especially if the depth of clay levels is shallow.

5.2.1 Sodium percentage

The sodium percentage was calculated to provide information about the suitability of groundwater for irrigation, as excess sodium can result in reduced soil permeability (Janardhana Raju et al. 1992; Wilcox 1955). In fact, high %Na in groundwater (above 60%) may cause sodium accumulations which will engender a disturbance of soil structure (Fipps 2003). The %Na of the Mornag groundwater samples varies from 24.7 to 66.3%

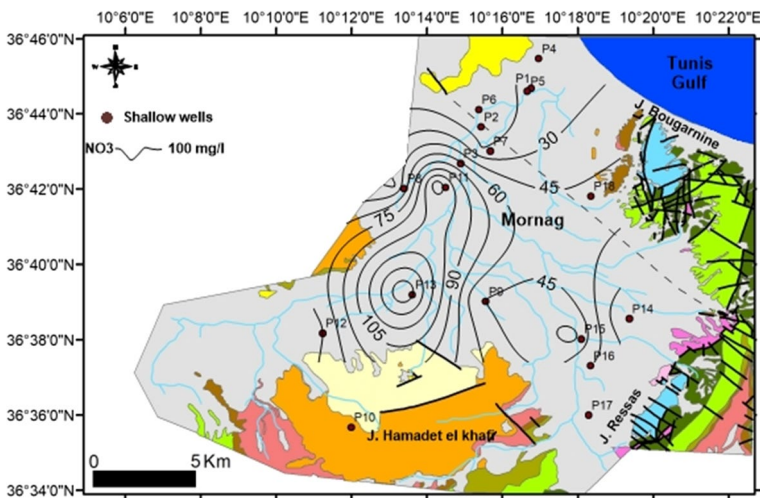


Fig. 13 Spatial distribution of nitrate

with a mean value of 46.04%. It has been displayed that 77.7% samples are permissible to suitable for irrigation. However, about 23% of groundwater samples are classified as doubtful for irrigation (Table 3).

According to the Wilcox diagram, which represents the evolution of sodium percent with respect to EC, the Mornag groundwater samples have been classified into three different categories. About 28% of groundwater samples, collected from wells located in the recharge area, fall in the “Good to Permissible” category, suggesting a low mineralization (Figs. 14, 15). Only 18% of samples fall in the category “Doubtful to Permissible,” indicating medium mineralization. Almost half of groundwater samples (55%) fall into the category of unsuitable for irrigation purposes, highlighting high mineralization ($EC > 3000 \mu\text{s/cm}$). This classification suggests that the great majority of groundwater, sampled from the central and northern parts of the Mornag plain, is unsuitable for irrigation purposes, which can result in reduced soil permeability and consequently generate poorly drained soils (Fig. 15).

5.2.2 Permeability index (PI)

The soil permeability index is largely influenced by the chemical composition of soil and irrigation water (sodium, calcium, magnesium and bicarbonate). This parameter, which was calculated using the following formula, has been estimated to assess the suitability of groundwater for irrigation (Doneen 1964).

The permeability index of Mornag shallow groundwater varies from 35.9 to 68.55% (Table 3). Based on this parameter (PI), waters can be classified into three classes I, II, and III (Doneen 1964). Waters are considered as suitable to good for irrigation if they belong to the classes I and II with 25–75% of maximum permeability. For those belonging to class III, waters are judged as unsuitable for irrigation purpose with 25%

Table 3 Calculated values of sodium percentage (%Na), permeability index (PI) and sodium adsorption ratio (SAR) to assess the suitability of groundwater samples for irrigation

Well number	%Na	%PI	SAR
P1	76.77	68.55	8.92
P2	72.66	65.28	8.65
P3	73.98	64.26	10.01
P4	75.76	65.55	6.96
P5	58.88	58.08	9.46
P6	49.54	51.22	7.96
P7	48.34	53.72	5.17
P8	76.73	68.30	4.59
P9	48.69	52.81	3.64
P10	56.18	39.24	4.62
P11	51.96	51.84	7.99
P12	50.10	51.60	2.84
P13	57.01	37.42	2.60
P14	42.95	41.10	1.35
P15	79.36	66.94	21.75
P16	46.07	48.69	4.18
P17	34.39	35.97	2.17
P18	61.71	51.90	2.12

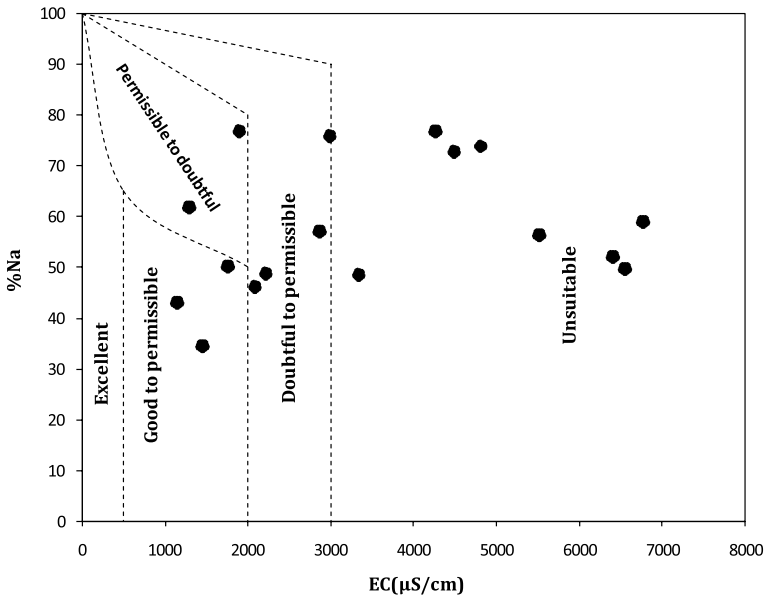


Fig. 14 The quality of groundwater in relation to electrical conductivity and percent sodium (Wilcox diagram)

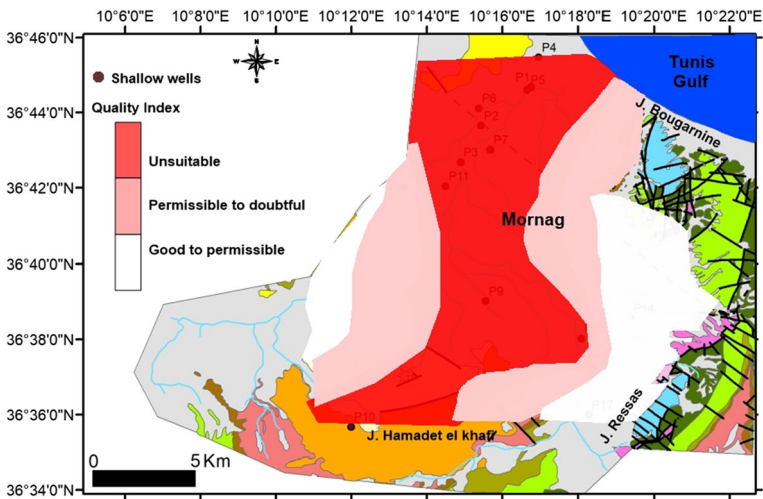


Fig. 15 Spatial distribution map of water quality index

of maximum permeability. In the present investigation, the Doneen classification shows that all the groundwater samples fall in class I, suggesting that the Mornag shallow groundwaters were acceptable to good for irrigation use.

5.2.3 Sodium adsorption ratio (SAR)

Sodium adsorption ratio (SAR) is another index of evaluation of the water suitability for agricultural irrigation use. Indeed, high SAR can result in a reduction in the permeability and structure of soil (Todd and Mays 2005; Hussein 2017). Moreover, under arid climatic condition, this may engender a lot of problems such as soils salinization which affects the capacity of plants through the roots and poor drainage conditions (Hem 1985).

The Mornag groundwater samples show SAR values varying between 1.34 and 21.75 with an average value of 6.38 (Table 3). About 89% of the studied samples, located mainly in the foot of the surrounding hills, display SAR values below 10, indicating an excellent irrigation water quality and consequently little danger (Fig. 16). Eleven percentage of groundwater samples, collected from wells situated in the center and the north of the plain, show SAR values above 10, suggesting precipitation induced by leaching and dissolution of salts and therefore can cause soil texture degradation and influence plant survival and growth (Richards 1954). Basing on the plot of SAR versus electrical conductivity (US salinity diagram), groundwater samples were classified into different categories (Wilcox 1948) (Fig. 17). This diagram displays that 45% of samples correspond to the C_3-S_1 and C_3-S_2 classes, highlighting high salinity and low to medium SAR. However, 28% of samples belong to the C_4-S_1 and C_4-S_2 classes, indicating elevated salinity and medium sodium hazard. Furthermore, 28% of water samples fell in the C_3-S_1 category, highlighting very high salinity and high sodium hazard. To conclude, samples that fall in C_4-S_1 , C_4-S_2 and C_4-S_3 are considered to be unsuitable for irrigation purpose in all soil types, except for highly permeable soil with large capacity of drainage and the selection of plants with good salt tolerance (Kumar et al. 2007). In fact, the application of these water types in irrigation will engender decline in yield crop and deteriorate the soil structure and texture. However, groundwater samples that fall in the C_3-S_1 category should only be used to irrigate salt-tolerant crops grown on well-drained soils with high permeability under regular monitoring of the evolution of salinity (Salifu et al. 2013).

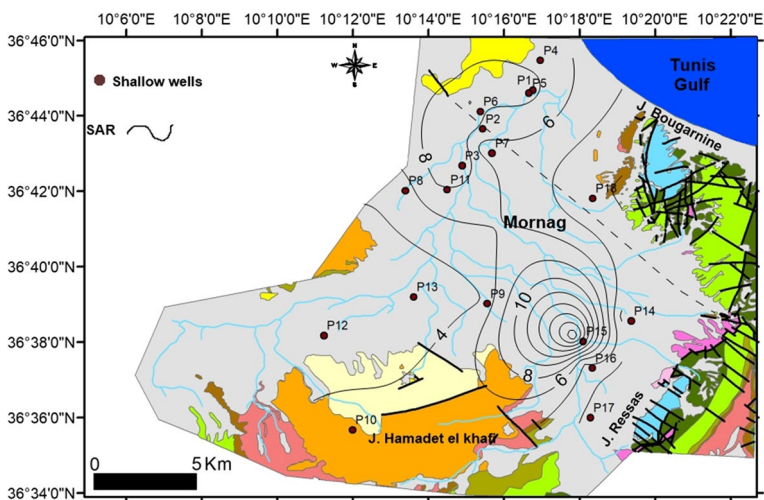


Fig. 16 Spatial distribution map of SAR values in the Mornag groundwaters

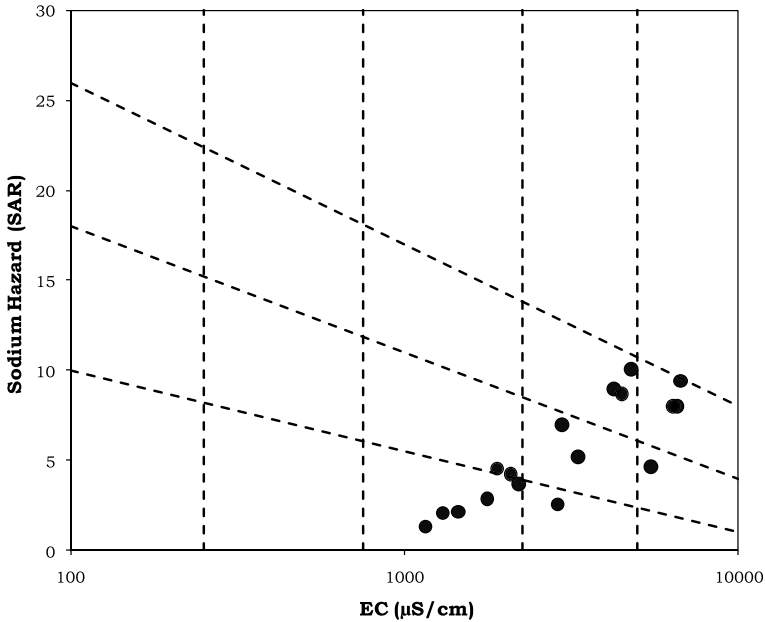


Fig. 17 The quality of groundwater in relation to salinity and sodium hazard

6 Conclusion

In semiarid regions of the developing countries, natural and anthropogenic processes that affect water quality constitute the main threat to groundwater sustainability. The hydrochemical composition of the Mornag quaternary groundwaters has been investigated to recognize the main processes governing their quality and to assess their suitability for irrigation. The major ions contents were examined to evaluate the quality groundwater through the identification of the mineralization processes. Groundwater quality indexes (PI, %Na, SAR) were used to assess the groundwater suitability for irrigation purpose. In order of abundance, from highest to lowest, the abundant ions are $\text{Na}^+ > \text{Ca}^{2+} > \text{Mg}^{2+} > \text{K}^+$ and $\text{Cl}^- > \text{SO}_4^{2-} > \text{HCO}_3^- > \text{NO}_3^-$. It has been demonstrated that $\text{Cl-SO}_4\text{-Ca}$ and Na-Cl water types are the result of water-rock interaction processes such as the evaporite dissolution (halite, gypsum and/or anhydrite) and reverse ion exchange. The irrigation water quality index calculated within this framework showed that the Mornag groundwaters have a high electrical conductivity, high sodium hazard ($\text{C}_4\text{-S}_1$, $\text{C}_4\text{-S}_2$ and $\text{C}_4\text{-S}_3$) and relatively high permeability index, suggesting that the quality of the Mornag shallow groundwater is generally unsuitable for irrigation. The long-term use of these resources of irrigation may increase the salinity and permeability problems in the soils. The sustainable management of groundwater resources must play a critical role in solving water scarcity problems. In fact, local management of groundwater will contribute to decentralization of decision and permit to farmers to take essential part in the decisions that define the future prospects of their agricultural lands and the water resources quality. This is through the integration of new knowledge to promote sustainable and efficient management of groundwater and soil resources.

Acknowledgements We would like to express our gratitude to staff of the “Laboratoire de Radio-Analyses et Environnement (LRAE)” of the Engineers School of Sfax, Tunisia, for their help in providing geochemical analysis.

References

- Amin, B. M., Wani, A. S., Vijay, K., Jyotirmaya, S., & Dinesh, T. (2018). An overview of the assessment of groundwater quality for irrigation. *Journal of Agricultural Science and Food Research*, 9, 209.
- Amri, A., Ben Fadhel, M., Chermiti, A., & Ben Youssef, M. (2018). Biostratigraphy of upper Cretaceous through Paleocene successions in Grombalia, Tunisia (southern Tethyan domain)—Reworking processes and interpretations. *Arabian Journal of Geosciences*, 11, 253.
- Bargaoui, Z. (1983). Contribution à l'étude statique de la pluie dans la région de Tunis. Thèse de Doctorat ingénieur, Institut Nationale Polytechnique de Toulouse.
- Ben Haj Ali, M., Jedoui, Y., Dali, T., Ben Salem, H., & Memmi, L. (1985). Geological map of Tunisia at the scale 1/500,000, ed. Serv. Géol., Tunisia.
- Biely, A., Rakus, M., Robinson, P., & Salaj, J. (1972). Essai de corrélation des formations miocènes au Sud de la dorsale tunisienne. *Notes du Service Géologique de Tunisie*, 38, 73–93.
- Bismuth, H., & Hooyberghs, H. J. F. (1994). Foraminifères planctoniques et biostratigraphie de l'Oligocène et du Néogène dans le sondage de Korba 1 (Cap Bon, Tunisie nord-orientale). *Bulletin des Centres de Recherches Exploration Production Elf-Aquitaine*, 18, 489–528.
- Bonnefous, J. (1972). Contribution à l'étude stratigraphique et micro paléontologique du Jurassique de Tunisie (Tunisie septentrionale et centrale, Sahel, zone des chotts). Thèse doct. es-sciences naturelles (Vol. VI, p. 397). University of Paris.
- Bouhleb, S. (1982). Distribution du baryum et du strontium dans les gisements de la province fluorée tunisienne; application aux gites de Hammam Djedidi et Hammam Zriba-Jebel Guebli. Thèse de doctorat de 3ème cycle. Université de Paul Sabatier de Toulouse, France.
- BRLI ingénierie. (2007). Projet d'amélioration de la gestion intégrée des périmètres irrigués de Mornag. Etude de factibilité. BRLi, p. 22.
- Bujalka, P., Vacek, J., & Rakus, M. (1971). Geological map of La Goulette at the scale 1/50,000, ed. Serv. Géol. Tunisia.
- Burrollet, P. F. (1956). Contribution à l'étude stratigraphique de la Tunisie centrale. *Annales des mines et de la géologie Tunisie*, 18, 350.
- Chandoul, S. (2017). Apports des outils géochimiques et isotopiques à l'identification des origines de la minéralisation des eaux de la nappe phréatique de Mornag (Gouvernorat de BEN AROUS). Master, Université de Sfax, p. 106.
- Dassi, L., Zouari, K., & Faye, S. (2005). Identifying sources of groundwater recharge in the Merguellil basin (Tunisia) using isotopic methods: Implication of dam reservoir water accounting. *Environmental Geology*, 49, 114–123.
- Domenico, P. A., & Schwartz, F. W. (1990). *Physical and chemical hydrogeology* (pp. 410–420). New York: Wiley.
- Doneen, L. D. (1964). Notes on water quality in agriculture published as a water science and engineering paper 4001. Department of Water Science and Engineering, University of California.
- Ennabli, M. (1980). Etude hydrogéologique des aquifères du Nord-Est de la Tunisie pour une gestion intégrée des ressources en eau. Thèse de doctorat d'Etat, Université de Nice, p. 72.
- Farhat, S. (2011). Caractérisation de la géométrie des aquifères Mio-plio-quadernaires de la plaine de Mornag (en Tunisie) par les méthodes géophysiques. Hydrochimie et modélisation de la recharge potentielle. Thèse de Doctorat, Faculté des Sciences de Tunis, Département de géologie, p. 208.
- Fipps, G. (2003). Irrigation water quality standards and salinity management strategies. Texas Agricultural Extension Service, Texas A&M University System, College Station, TX (USA). B-1667, 4-03, pp. 1–19.
- Florida, S., & Massin, J. M. (1969). Contribution à l'étude des extrusions jurassiques de la Tunisie septentrionale. Etude géologique et minière du secteur d'Hammam Djedidi. *Bulletin de la Société Géologique de France*, 7, 82–97.
- Freeze, R. A., & Cherry, J. A. (1979). *Groundwater*. Upper Saddle River: Prentice Hall.
- Gibbs, R. J. (1970). Mechanisms controlling world water chemistry. *Science*, 170, 1081–1090.
- Hechemi, H. (1989). *carte des ressources en eau de la Tunisie au 1/200 000. Notice explicative* (p. 19). Tunis: DGRE.

- Hem, J. D. (1985). Study and interpretation of the chemical characteristics of natural water (3rd ed.). US Geological Survey Water- Supply Paper 2254, p. 263.
- Hussein, B. G. (2017). Groundwater chemistry evaluation for drinking and irrigation utilities in east Wasit province, Central Iraq. *Applied Water Science*, 7, 3447–3467.
- Janardhana Raju, N., Reddy, T. V. K., & Kotaiah, B. P. T. (1992). A study on seasonal variations of ground water quality in Upper Gunjanaeru River basin, Cuddapah District, Andhra Pradesh. *Fresenius Environmental Bulletin*, 1, 98–103.
- Kalaivanan, K., Gurugnanam, B., Pourghasemi, H. R., Suresh, M., & Kumaravel, S. (2018). Spatial assessment of groundwater quality using water quality index and hydrochemical indices in the Kodavanan sub-basin, Tamil Nadu, India. *Sustainable Water Resources Management*, 4(3), 627–641.
- Kamel, S., Dassi, L., & Zouari, K. (2006). Approche hydrogéologique et hydrochimique des échanges hydrodynamiques entre aquifères profond et superficiel du bassin du Djérid, Tunisie. *Hydrological Sciences Journal*, 51(4), 713–730.
- Kumar, M., Kumari, K., Ramanathan, A., & Saxena, R. (2007). A comparative evaluation of groundwater suitability for irrigation and drinking purposes in two intensively cultivated districts of Punjab, India. *Environmental Geology*, 53, 553–574.
- Lajmi, T. (1968). Contribution à l'étude géologique et hydrogéologique de la plaine de Mornag. Notes du service géologique N°27 (p. 7). Tunis: DGRE.
- Lassoued, B., Labbene, H., & Gouider, N. (1995). Note sur l'exploitation du système aquifère de Mornag. Tunis: DGRE.
- Mezrioui, I. (2015). Qualité des eaux de la nappe de Mornag et Vulnérabilité à la pollution. Mémoire de Mastère, FST Tunis, pp. 21–22.
- Moussa, A. B., Bel Haj Salem, S., Zouari, K., & Jelassi, F. (2017). Hydrochemical and stable isotopic investigation of groundwater quality and its sustainability for irrigation in the Hammamet-Nabeul basin, northeastern Tunisia. *Arabian Journal of Geosciences*, 10, 446.
- Moussa, A. B., Mzali, H., Zouari, K., & Hezzi, H. (2014). Hydrochemical and isotope assessment of groundwater quality in the quaternary shallow aquifer, Tazoghane region, north-eastern Tunisia. *Quaternary International*, 338(4), 51–58.
- Moussa, A. B., & Zouari, K. (2011). Hydrochemical investigation of groundwater contamination in the Grombalia shallow aquifer, Cap Bon Peninsula, Tunisia: Impact of irrigation with industrial waste water. *Waste Water—Evaluation and Management*, 11, 239–252.
- Moussa, A. B., Zouari, K., & Oueslati, N. (2008). Geochemical study of groundwater mineralization in the Grombalia shallow aquifer, north-eastern Tunisia: Implication of irrigation and industrial waste water accounting. *Environmental Geology*, 58(3), 555–566.
- Mzali, H., & Zouari, H. (2012). Structural cutting of a region showing various compound tectonic deformations (example of Bouficha-Grombalia region). *Arabian Journal of Geosciences*, 5, 13.
- Piper, A. M. (1944). A geographic procedure in the geochemical interpretation of water analysis. *Transactions of the American Geophysical Union*, 25, 914–923.
- Rakus, M., & Biely, A. (1971). Stratigraphie du Lias dans la Dorsale tunisienne, Notes Serv. Géol. Tunisie, Tunis, no. 32, 45–63.
- Richards, L. A. (1954). *Diagnosis and improvement of saline alkali soils: agriculture, handbook* (Vol. 160, p. 60). Washington DC: US Department of Agriculture.
- Salifu, M., Yidana, S. M., Osa, S., & Armah, Y. S. (2013). The influence of the unsaturated zone on the high fluoride contents in groundwater in the Middle Voltaian aquifers—The Gushegu District, Northern Region of Ghana. *Journal of Hydrogeology and Hydrologic Engineering*, 2, 2.
- Soussi, M., Mangold, C., Enay, R., Boughdiri, M., & Ben Ismail, M. H. (2000). Le Jurassique inférieur et moyen de la Tunisie septentrionale; corrélations avec l'Axe Nord-Sud et paléogéographie. *Geobios*, 33, 437–446.
- Tarki, M., Ben Hammadi, M., El Mejri, H., & Dassi, L. (2016). Assessment of hydrochemical processes and groundwater hydrodynamics in a multilayer aquifer system under long-term irrigation condition: A case study of Nefzaoua basin, southern Tunisia. *Applied Radiation and Isotopes*, 110, 138–149.
- Todd, D. K., & Mays, L. W. (2005). *Groundwater hydrology* (3rd ed., p. 656). Hoboken, NJ: Wiley.
- Toumi, N., Hussein, B. H., & Rafrafi, S. (2015). Groundwater quality and hydrochemical properties of Al-Ula region, Saudi Arabia. *Environmental Monitoring and Assessment*, 187, 84.
- Turki, M. M. (1985). Polycinématique et contrôle sédimentaire associé sur la cicatrice Zaghuan-Nebhana. Es-sciences doctorate thesis. El Manar University, p. 262.
- Vacek, J., Krivy, M., Johan, Z., Bujalka, P., & Rakus, M. (1971). Geological map of Grombalia at the scale 1/50 000, ed. Serv. Géol. Tunisie.

WHO. (2011). Guidelines for drinking-water quality. *World Health Organization*, 216, 303–304.

Wilcox, L. V. (1948). The quality of water for irrigation use. United States Department of Agriculture, Economic Research Service.

Wilcox, L. V. (1955). Classification and use of irrigation water. USDA, Circular 969, Washington, DC, p. 19.

Publisher's Note Springer Nature remains neutral with regard to jurisdictional claims in published maps and institutional affiliations.

Affiliations

Amor Ben Moussa^{1,2,3} · Sawsan Chandoul² · Houcem Mzali⁴ · Sarra Bel Haj Salem¹ · Hatem Elmejri¹ · Kamel Zouari⁵ · Amor Hafiane² · Habib Mrabet⁶

¹ Research Laboratory of Environmental Science & Technologies, Borj Cedria, Tunisia

² Eau-Membrane et Biotechnologie de l'Environnement, CERTE, Borj Cedria, Tunisia

³ High Institute of Environmental Science and Technology (HIEST) of Borj Cedria, Borj Cedria, Tunisia

⁴ Laboratoire de Géoresources, Centre de Recherches et Technologies des Eaux, BP 273, 8020 Soliman, Tunisia

⁵ Laboratory of Radio-Analyses and Environment, National School of Engineers of Sfax, University of Sfax, BP 1173, 3038 Sfax, Tunisia

⁶ Commissariat Régional au Développement Agricole de Ben Arous, Ben Arous, Tunisia